Quenching of the Nonlocal Electron Heat Transport by Large External Magnetic Fields in a Laser-Produced Plasma Measured with Imaging Thomson Scattering

D. H. Froula,* J. S. Ross, B. B. Pollock,† P. Davis,‡ A. N. James,† L. Divol, M. J. Edwards, A. A. Offenberger,§ D. Price, R. P. J. Town, G. R. Tynan,† and S. H. Glenzer

L-399, Lawrence Livermore National Laboratory, P.O. Box 808, Livermore, California 94551, USA

(Received 24 May 2006; published 29 March 2007)

We present a direct measurement of the quenching of nonlocal heat transport in a laser-produced plasma by applying large external magnetic fields (>10 T). The temporally resolved Thomson-scattering measurements of the electron temperature profile show that the heat front propagation transverse to a high-power laser beam is slowed resulting in extremely strong local heating. We find agreement with hydrodynamic modeling when including a magnetic field model that self-consistently evolves the fields in the plasma.

DOI: 10.1103/PhysRevLett.98.135001 PACS numbers: 52.25.Os, 52.35.Fp, 52.50.Jm

Inertial confinement fusion (ICF) and high energy density science (HEDS) experiments require a detailed understanding of heat transport in the presence of magnetic fields [1]. The indirect drive approach to ICF requires a detailed understanding of the plasma conditions in the presence of magnetic fields to accurately predict laser beam propagation [2]. Cross-magnetic-field heat transport is also important for understanding magnetic fusion plasmas, astrophysical observations [3], and basic plasma physics [4].

Current hydrodynamic simulations used to design ignition hohlraums typically employ a flux-limited thermal diffusion model. In this model the heat flux is determined from the minimum of the classical Spitzer-Härm (SH) value and the free-streaming value (limited by a *flux limiter*) [5]. The flux limiter was introduced primarily to reproduce experiments where simulations involve energy transport from the laser absorption region into a solid target [6]. However, the coronal plasmas have been difficult to model even though SH diffusion has been successfully applied in a number of experiments that employ gas targets without a critical surface [7]. The SH heat flow depends on the local temperature gradients and is thus referred to as a local model. This local approximation breaks down in steep temperature gradients and a nonlocal model should be used that take account of the non-Maxwellian nature of the electron velocity distribution. In addition, the steep density and temperature gradients typically found in laser-generated plasmas can lead to self-generated magnetic fields [8] that may act to localize the heat flow. Currently, there are outstanding questions regarding the relative importance of nonlocal heat transport [9] and the effects of self-generated magnetic fields in the complex hohlraum plasmas employed in ICF; furthermore, in laser-produced plasmas there are no direct measurements of electron heat transport in the presence of magnetic fields to compare with modeling calculations.

In this Letter, we present the first observation of the localization of the electron heat transport by high magnetic fields in high temperature laser-produced plasmas. It is found that a 12 Tesla external magnetic field oriented parallel to a high-power laser beam inhibits electron thermal transport perpendicular to the heater beam, reducing the heat flux by a factor of $\kappa_{\parallel}/\kappa_{\perp} = 15$, where $\kappa_{\parallel}$, $\kappa_{\perp}$ are the conductivities parallel and perpendicular to the magnetic field, respectively. With this reduction in heat flux, simulations show the plasma expands adiabatically. Since the magnetic Reynold's number is large, the magnetic field is frozen into the plasma and as the plasma expands ($\beta =$ plasma/magnetic pressure $= 20$) the magnetic field follows the density and is compressed at the heat front.

Spatially and temporally resolved temperature measurements using imaging Thomson scattering provide data for a critical test of hydrodynamic simulations that include magnetic fields. We find for the highest imposed magnetic fields ($B = 12$ T) that the electrons of the plasma gyrate with a Larmor radius ($r_c = mv/eB = 5\ \mu$m) that is smaller than the temperature scale length ($T_e/\nabla T_e \simeq 300\ \mu$m), thereby localizing the electron flux ($r_c \ll T_e/\nabla T_e$) and classical Braginskii heat transport is successful in modeling the heat wave propagation. This results in very large central electron temperatures, a factor of 4 higher than without applying the external field. This finding indicates that the presence of magnetic fields has important consequences for the temperature profile in laser-produced plasmas suggesting that self-generated magnetic fields need to be included in integrated simulations of laser-plasma experiments where large magnetic fields are generated. The results from this experiment will provide valuable data for comparing to new hydrodynamic simulations that implement both nonlocal and magnetic field models [10].

This experiment was performed in the Janus Laser Facility at the Lawrence Livermore National Laboratory (Fig. 1). Plasmas were produced in a nitrogen gas jet with a 1.5 mm diameter cylindrical nozzle and an operating upstream pressure of 6.5 atm. The opening of the nozzle was aligned 1.5 mm below the target chamber center (TCC). The neutral gas density was well characterized using interferometery [11]; the peak electron density for our con-

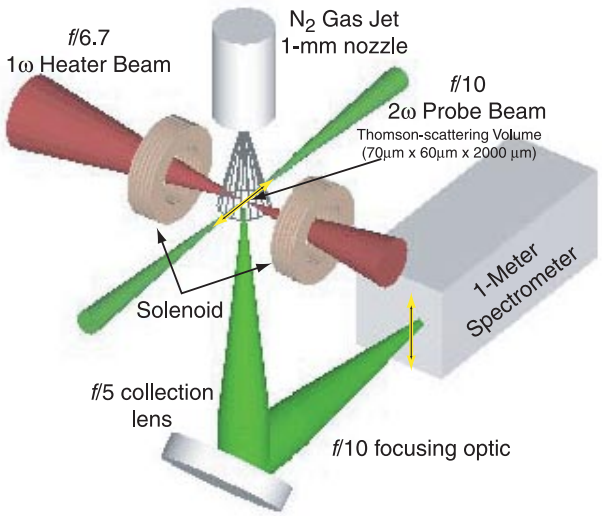

FIG. 1 (color). The experimental setup is shown where a 1ω high-power (1-ns square) laser beam initially heats a narrow 200 μm plasma channel in N_2 gas injected by a 1.5 mm nozzle. Two solenoids produce a uniform high magnetic field ($B =$ 12 Tesla) parallel to the heater beam. A collective Thomson-scattering diagnostic measures the electron temperature profile perpendicular to the heater beam using a low power 2ω probe; a spectrometer slit is imaged perpendicular to the heater beam to collect light scattered from the low energy 2ω probe laser.

ditions (fully ionized nitrogen) was $n_e = 1.5 \times 10^{19}\ \mathrm{cm}^{-3}$. A 1ω (1054 nm), 100 J laser beam was focused with a 1 m focal length lens ($f/6.7$) through a continuous phase plate producing a 150 μm diameter focus at TCC. The laser pulse was 1-ns square with a 350 ps rise and fall measured to the half intensity point.

A second laser beam, frequency doubled (2ω) to produce 0.5 J in 200 ps, was used to probe the plasma perpendicular to the high-power beam by focusing the laser light with a 40 cm focal length lens ($f/10$) to a 70 μm diameter spot at TCC. The Thomson-scattered light was collected at an angle of 90° and collimated by an $f/5$ lens and imaged with a $f/15$ focusing lens on to the 200 μm entrance slit of a 1 m, 2400 groves/mm imaging spectrometer. The Thomson-scattering collection system had a magnification of 3. An intensified gated CCD camera with 26 μm square pixels was coupled to the spectrometer providing a spectral resolution of $\delta\lambda = 0.09$ nm and a spatial resolution perpendicular to the high-power heater beam better than $\delta x = 30$ microns.

The Thomson-scattering volume was defined by the beam waist of the probe laser (70 μm diameter) and the projection of the spectrometer slit into the plasma plane. The time between the beams was varied to study the temporal evolution of the plasma heating; the relative beam timing was known to 200 ps.

An external magnetic field parallel to the heater beam was generated by driving high currents through a modified Bitter magnet [12]. The magnet was driven with a pulsed power system capable of delivering a peak current of 15 kA, resulting in a 12 T field in vacuum at the TCC. The magnetic field was shown to be constant over the laser experiment scale lengths (~1 mm, 1 ns) [13].

Figure 2 compares the Thomson-scattering spectra for $B = 0$ T and $B = 12$ T; the separation between the spectral features ($\Delta\lambda$) is a direct measure of the electron temperature. In Fig. 2 we clearly observe that the transverse thermal heat front propagation has been inhibited. For $B = 12$ T, the hot plasma extends spatially from -0.3 mm to $+0.3$ mm compared to -0.7 mm to $+0.7$ mm in the unmagnetized case. Moreover, the wavelength separation between the ion-acoustic features inside of the heated plasma region is significantly larger with an external magnetic field of 12 T indicating strong local heating ($\Delta\lambda_{B=12}/\Delta\lambda_{B=0} \simeq 2$; $T_{B=12}/T_{B=0} = 4$). The electron temperature profile is obtained by fitting the measured frequency spectrum every 30 microns with the frequency-dependent Thomson-scattering form factor $S(k, \omega)$ [14]. The average ionization state is calculated using a Thomas-Fermi model giving Z in the range of 4–7 for the electron temperature between $T_e = 20$ eV and $T_e = 350$ eV [9]. Including errors in the calculation of Z, the absolute temperature at $x = 0$ is determined to within an accuracy of 15%. The asymmetry around the heater beam observed in

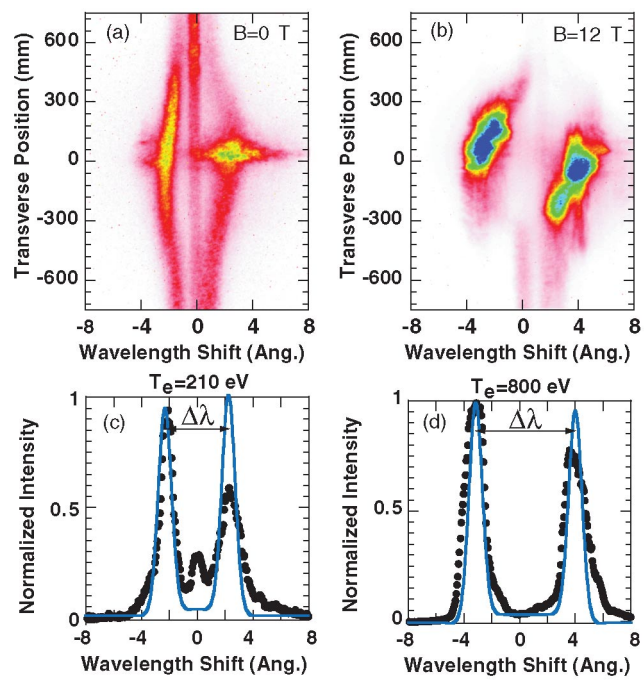

FIG. 2 (color). Spatially resolved Thomson-scattering spectra are presented for conditions: (a) without an external magnetic field ($B = 0$ T) near the end of the heating pulse and (b) with a high magnetic field ($B = 12$ T), 500 ps after the end of the heater; the magnetic field reduces the spatial extent of the plasma and increases the electron temperature by a factor of 4. The spectra near the center of the heated region are shown for both conditions (c) $B = 0$ T ($T_e = 210$ eV), (d) $B = 12$ T ($T_e =$ 800 eV); data are fit with a form factor to determine the electron temperatures from the separation between the spectral features.

the Thomson-scattering spectrum is a result of the convolution of the gradients in the frequency shifts of both the sound speed and radial plasma flow associated with plasma expansion.

Figure 3 shows the heat wave propagation for the highest magnetic field experiments ($B = 12$ T). These match simulations using the hydrodynamic code LASNEX [5] used to solve the classical heat transport equations originally presented by Braginskii [15]. In this comparison it is evident that a 12 Tesla magnetic field is sufficient to localized the electron heat flux ($v_e \tau_c < T_e/\nabla T_e$) and the measurements are well reproduced without invoking "turbulent" transport models ($r_c \gg \lambda_{De}$) which is required in most magnetic fusion energy research due to nonthermal fluctuations such as unstable waves or gradient driven broad band turbulence.

In our $B > 0$ magnetic field fluid simulations the electron heat flux is determined by the minimum between the Braginskii heat flux (q_B) and the free-streaming heat flux ($q_{fs} = n_e T_e v_e$);

$$\mathbf{q}_B = -\kappa_\parallel \nabla_\parallel T_e - \kappa_\perp \nabla_\perp T_e, \tag{1}$$

where the cross-thermal conductivities have been neglected due to the axisymmetry of the experiment and the conductivities can be approximated for the high magnetic field simulations by [16,17]

$$\kappa_\parallel = 3.2\frac{Zn_e T_e \tau_{ei}}{m_e}; \qquad \kappa_\perp = 4.7\frac{Zn_e T_e \tau_{ei}}{m_e \omega_{ce}^2 \tau_{ei}^2}.$$

Comparing the conductivity effected by the external magnetic field ($\kappa_\perp$) with the conductivity that is not affected by the external magnetic field ($\kappa_\parallel$) provides an estimate of the reduction in heat flux for a 10 T magnetic field, $\kappa_\parallel/\kappa_\perp = 15$.

Our LASNEX simulations propagate a laser pulse, using the experimental parameters, through a constant density two-dimensional slab (1.5×10^{19} cm^{-3}). The external magnetic field is imposed around the beam (B_θ field) in order to take advantage of the ability of LASNEX to self-consistently calculate the evolution of such a magnetic field. Potentially this field orientation (B_θ) could limit the heat flux in the direction of the laser beam, but for our conditions the heater beam efficiently heats the neutral gas along the beam path and there is no parallel temperature gradient to drive a heat flux.

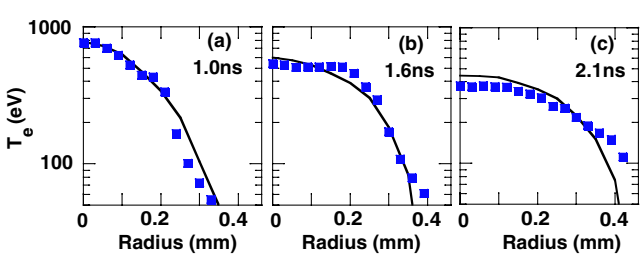

FIG. 3 (color online). A series of measured electron temperature profiles (a) 1.0 ns, (b) 1.6 ns, (c) 2.1 ns are compared to the simulated temperatures using the Braginskii model (curves) showing that the heat wave has been localized by a $B = 12$ T magnetic field.

Figure 4(a) compares the electron temperature profiles with and without a magnetic field 1 ns after the rise of heater beam. The profile obtained without an external magnetic field ($B = 0$ T) shows that the heat front extends out well past 500 microns from the center of the heater beam. The $B = 0$ results are reproduced by full nonlocal simulations using the code SPARK [18] that solves 1D Fokker-Plank equations in the diffusion approximation, consistent with earlier work [9]. The measurements shown in Fig. 4(a) are direct evidence for the reduction in electron heat flux by an external magnetic field and the reduction in the heat wave propagation shows the quenching of the nonlocal heat transport by externally applied magnetic fields.

Figure 4(b) compares the measured electron temperature at 1 ns with the hydrodynamic simulations for different external magnetic fields. As the magnetic field is reduced, the Larmor radius becomes comparable to the scale length of the electron temperature gradient and the nonlocal nature of the plasma becomes important in simulating the electron temperature. This may be evident in the low field measurements ($B < 10$ T) where the simulations slightly overestimate the electron temperature; when no magnetic field is applied, nonlocal simulations are required to reproduce the results [Fig. 4(a)] [9].

For our conditions, the magnetic field serves to restrict the electron thermal conduction losses but it is not sufficient to confine the hot plasma to the laser-heated core ($\beta \simeq 20$). Initially the simulations show a background magnetic field throughout the plasma. At 1.5 ns, the field

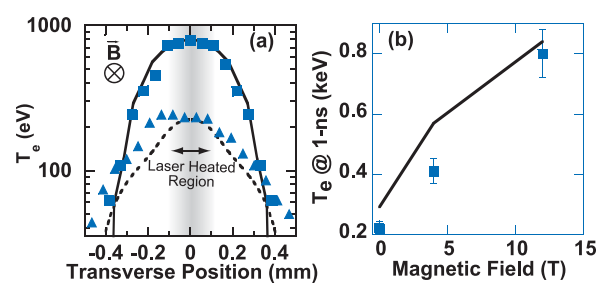

FIG. 4 (color online). (a) The electron temperature profiles for no magnetic field (triangles) and an externally applied field of 12 Tesla (squares) show an increase in peak electron temperature and a corresponding reduction in the propagation of the heat wave perpendicular to the magnetic field lines. LASNEX simulations with an imposed self-consistent magnetic field reproduce the experimental results (solid-curve) when high external magnetic fields are applied. When no magnetic filed is imposed, a nonlocal model is required and reproduces the results (dashed-curve). (b) Comparison of the Braginskii model (curve) agrees well with the peak electron temperature measured (squares) when the maximum external magnetic field is applied ($B = 12$ T). For low magnetic field conditions, $B = 0$ T and $B = 4$ T, the model differs from the measurements indicating that nonlocal effects are important.

at the center of the plasma drops from the vacuum field of 12 T to 6 T, while the field at the heat front is compressed to nearly 16 T. This compression of the density and magnetic field is not sufficient to reach a balance between the magnetic field and the plasma pressure ($\beta \gg 1$) as a density compression greater than 20 is required. Turning off the magnetic field pressure in the simulations did not significantly change the results, indicating only energy confinement is important, further suggesting $\beta \gg 1$ conditions throughout the experiment.

The magnetic field compression closely follows the radial density compression due to the expanding plasma; initially, the magnetic field is trapped in the plasma, but as the temperature gradient resulting from the local laser beam heating creates a pressure gradient lowering the density in the center of the plasma, the field is pulled out by plasma expansion and compressed at the heat front. The evolution of the magnetic field can be derived from Ohm's law. The magnetic field convects with the flow and diffuses due to joule heating;

$$\frac{\partial B_z}{\partial t} - \nabla \cdot (\mathbf{v} B_z) = \frac{\eta}{\mu_0} \nabla^2 \mathbf{B}, \tag{2}$$

where $\eta_\perp \sim 1 \times 10^{-4} Z \ln(\Lambda)/T_{eV}^{3/2}$ is the plasma resistivity and $\ln(\Lambda) \sim 8$ is the Coulomb logarithm. Equation (2) shows that when the plasma resistivity is small (i.e., perfect conductor), magnetic field transport by convection greatly exceeds transport by diffusion and the magnetic field will be frozen into the expansion so that [19]

$$\frac{n_e(t)}{n_e(t=0)} \sim \frac{B(t)}{B(t=0)}. \tag{3}$$

Using the electron temperature ($T_e = 20$ eV) required to initially ionize the gas ($Z = 1$) and the scale length given by the transverse laser beam profile ($L \sim 100\ \mu$m), the diffusion time during the heating is estimated to be $\tau_d = \mu_0 L^2/\eta_\perp = 5.6$ ns. Therefore, during plasma formation which takes place over the rise time of the laser pulse ($\tau_L = 350$ ps), the magnetic field does not have time to diffuse ($\tau_L/\tau_d \ll 1$) before the resistivity can be neglected due to the rapid increase in electron temperature; consequently, the magnetic field is initially frozen into the plasma.

In summary, Thomson-scattering measurements have been successfully employed to demonstrate quenching of nonlocal heat transport in the presence of a large confining magnetic field. A 12 T external magnetic field parallel to a high-power laser beam is shown to reduce the heat flux by a factor of 15 when compared with hydrodynamic simulations using a Braginskii heat transport model. Fluid simulations using classical heat transport (i.e., no turbulence) in the presence of a magnetic field reproduce the measured heat wave propagation and increase in electron temperature in contrast to unmagnetized experiments which require a nonlocal treatment. The use of magnetic fields to contain the heat wave propagation has been shown to produce hot long scale-length plasmas that could be used for further studies on wakefield acceleration [20] and short-pulse amplification [21] that require long scale length, low density, hot plasmas.

We would like to acknowledge the efforts of the Janus Laser Crew. This work was performed under the auspices of the US Department of Energy by the Lawrence Livermore National Laboratory under Contract No. W-7405-ENG-48 and was partially supported by LDRD No. 06-ERD-056.

*Electronic address: froula1@llnl.gov
†Also at Department of Mechanical and Aerospace Engineering, Jacobs School of Engineering, and The Center for Energy Research, UCSD, University of California at San Diego, USA.
‡Also at Department of Engineering, University of British Columbia, Vancouver, Canada.
§Also at Department of Electrical Engineering, University of Alberta, Edmonton, Alberta, Canada T6G 2V4.

[1] P. Nicolai *et al.*, Phys. Plasmas **7**, 4250 (2000); M. G. Haines, Phys. Rev. Lett. **78**, 254 (1997); A. A. Offenberger and N. H. Burnett, Can. J. Phys. **53**, 1360 (1975).
[2] S. H. Glenzer *et al.*, Phys. Plasmas **6**, 2117 (1999).
[3] D. Ryutov *et al.*, Astrophys. J. **518**, 821 (1999).
[4] C. Driscoll *et al.*, Phys. Plasmas **9**, 1905 (2002).
[5] G. B. Zimmerman and W. L. Kruer, Comments Plasma Phys. Control. Fusion **2**, 51 (1975).
[6] C. A. Back *et al.*, Phys. Rev. Lett. **77**, 4350 (1996).
[7] S. H. Glenzer *et al.*, Nucl. Fusion **44**, S185 (2004); N. B. Meezan *et al.*, Phys. Plasmas **11**, 5573 (2004).
[8] J. Stamper, Laser Part. Beams **9**, 841 (1991).
[9] G. Gregori *et al.*, Phys. Rev. Lett. **92**, 205006 (2004).
[10] P. D. Nicolai *et al.*, Phys. Plasmas **13**, 032701 (2006).
[11] D. H. Froula *et al.*, Phys. Rev. Lett. **93**, 035001 (2004).
[12] F. Bitter, Rev. Sci. Instrum. **10**, 373 (1939).
[13] B. B. Pollock *et al.*, Rev. Sci. Instrum. **77**, 114703 (2006).
[14] J. A. Fejer, Can. J. Phys. **38**, 1114 (1960).
[15] S. I. Braginskii, Zh. Eksp. Teor. Fiz. **33**, 459 (1957).
[16] E. M. Epperlein and M. G. Haines, Phys. Fluids **29**, 1029 (1986).
[17] J. D. Huba, *NRL Plasma Formulary* (Naval Research Laboratory, Washington, DC, 2000).
[18] E. M. Epperlein *et al.*, Comput. Phys. Commun. **52**, 7 (1988); R. P. J. Town *et al.*, Phys. Rev. E **50**, 1413 (1994).
[19] N. H. Burnett and A. A. Offenberger, J. Appl. Phys. **45**, 2155 (1974).
[20] C. Geddes *et al.*, Nature (London) **431**, 538 (2004).
[21] N. J. Fisch and V. M. Malkin, Phys. Plasmas **10**, 2056 (2003).